Engineering Geology 264 (2020) 105335

Contents lists available at ScienceDirect

Engineering Geology

journal homepage: www.elsevier.com/locate/enggeo

Non-invasive time domain reflectometry probe for transient measurement of water retention curves in structured soils

Q.Y. Mu[a,b], L.T. Zhan[b,*], C.P. Lin[c], Y.M. Chen[b]

[a] Department of Civil Engineering, Xi'an Jiaotong University, Xi'an, 710049, China
[b] MOE Key Laboratory of Soft Soils and Geoenvironmental Engineering, Zhejiang University, Hangzhou, 310058, China
[c] Department of Civil Engineering, National Chiao Tung University, Hsinchu, 300, Taiwan

ARTICLE INFO

Keywords:
Water retention curve
Non-invasive TDR
Transient evaporation method
Structured soil

ABSTRACT

Transient evaporation method is promising for rapid measurement of soil water retention curve (WRC). Existing apparatuses of transient evaporation method are not ideal for measuring the WRC of structured soils because of the sample disturbance induced by invasive water content probes used. In this study, non-invasive TDR probes with different waveguide layouts (i.e., different number of conductors and waveguide length) were developed to measure the WRC of loess during transient evaporation, while the soil suction is recorded through a tensiometer. Results show that the WRCs of undisturbed and remolded loess measured by a three-conductor non-invasive TDR probe are in good agreement with the results of pressure plate tests. The differences in the air entry value (AEV) and desorption rate between the WRCs measured by the transient evaporation method and the pressure plate measurement are less than 10 %. On the other hand, the WRCs measured by a two-conductor non-invasive TDR probe underestimate the water content for a given suction. The AEV of undisturbed and remolded loess determined by the transient evaporation method is 66.7 % and 112.9 % smaller than the results of pressure plate measurements, respectively. The underestimation of the two-conductor non-invasive TDR probe in measuring the WRC of loess can be attributed to the fact that the vertical sampling range of two-conductor non-invasive TDR probe is two times greater than that of the tensiometer. The results in this study show the effectiveness of using the non-invasive TDR probe along with a tensiometer for measuring the WRC. More importantly, great caution should be taken on compliant sampling volume of the non-invasive TDR probe and tensiometer to obtain accurate WRC measurements.

1. Introduction

Water retention curve (WRC) is commonly described as the relationship between the soil suction and the volumetric water content (Fredlund and Rahardjo, 1993). Two fundamental properties of unsaturated soils (i.e., permeability and shear strength) that are widely associated with the geological disasters, such as the rainfall induced slope failure, can be derived from the WRC (Zhai and Rahardjo, 2015; Han and Vanapalli, 2016). On the other hand, the soil WRC is an important input parameter for the numerical computation of the water flow and the stability of the unsaturated soil slope (Xu et al., 2011; Hou et al., 2018; Cui et al., 2019). The methods that are commonly used for measuring the soil WRC in the laboratory involve equilibrating soil samples at prescribed suctions using axis translation, vapour equilibrium or osmotic techniques (Fredlund and Rahardjo, 1993). These methods are generally very time-consuming because of the extensive times required to achieve suction equilibrium between the soil sample and the instrument. To rapidly measure the soil WRC, the transient evaporation method was proposed in the literature (e.g., Rassam and Williams, 2000; Subedi et al., 2013) in which soil suction and volumetric water content are respectively measured by a tensiometer and a time domain reflectometry (TDR) probe during evaporation. However, existing apparatuses of transient evaporation method for measuring the WRC of structured soils are not ideal because of the sample disturbance induced by inserting the measurement probes.

Singh and Kuriyan (2003) developed a measurement cell, which consisted of a conventional TDR probe and a tensiomerter, to measure the soil WRC. The soil suction and volumetric water content measured by the tensiometer and TDR respectively were used to develop the soil WRC. Similar methods were also widely used to measure the soil WRC

* Corresponding author.
E-mail addresses: qingyimu@mail.xjtu.edu.cn (Q.Y. Mu), zhanlt@zju.edu.cn (L.T. Zhan), cplin@mail.nctu.edu.tw (C.P. Lin), chenyunmin@zju.edu.cn (Y.M. Chen).

https://doi.org/10.1016/j.enggeo.2019.105335
Received 4 April 2019; Received in revised form 6 October 2019; Accepted 11 October 2019
Available online 23 October 2019
0013-7952/

in the instantaneous profile test (Krisdani et al., 2009; Ng and Leung, 2011; Su et al., 2018). However, the conventional TDR probe measured average volumetric water content over a large soil volume along the conductors (e.g., > 10 cm), while the soil suction was measured in a soil volume adjacent to the small tensiometer. The large difference in sampling volumes of these two instruments may induce significant errors when developing the soil WRC (Vaz et al., 2002). To overcome this limitation, some researchers proposed new designs of TDR-tensiometer probe, which wraps conductor wires around a tensiometer (Vaz et al., 2002; Subedi et al., 2013). This kind of probe design allows the measurements of soil volumetric water content and suction within approximately the same soil volume around the combined probe. However, the soil sample must be penetrated to obtain the measurements, inevitably altering the micro-structure (e.g., pore size distribution) of the soil adjacent to the probe. The sample disturbance induced by the penetration of TDR probe results in an alternation of the water retention behaviour of structured soils, characterized by the special pore size distribution and arrangement of soil particles (Mitchell and Soga, 2005). As shown by some previous studies (Haeri et al., 2016; Ng et al., 2016), the air entry value (AEV) and hysteresis in the WRCs of the structured loess are significantly influenced by sample disturbance.

During the past several decades, many studies have been carried out to improve the design of TDR probes (Selker et al., 1993; Vaz et al., 2002; Lin et al., 2006; Zhan et al., 2015; Zhang et al., 2017; Mu et al., 2019). Among these studies, Selker et al. (1993) proposed to place serpentine waveguide on an acrylic plate to develop the non-invasive TDR probe. This type of probe design allows the measurement of soil volumetric water content without penetration. Nissen et al. (2003) introduced a similar design of non-invasive TDR probe implemented by metal-coated printed circuit board method. They reported that the water and solute transport can be well captured through measuring the soil volumetric water content and electrical conductivity with the non-invasive TDR probe. However, existing non-invasive TDR probes are not applicable to measure the WRC of structured soils through the transient evaporation method. It is mainly because that the compliant sampling volume of the TDR and the tensiometer was not considered in the current design of non-invasive probes.

In this study, a new cell was developed to measure the WRC of structured soils during transient evaporation. The measurement cell consists of two major components: a non-invasive probe (waveguide) and a tensiometer. The performance of different designs of waveguide was evaluated from the viewpoints of reflection waveform, measurement sensitivity, and sampling volume. The WRCs of loess, which falls into the category of structured soils, were measured through the cell equipped with a two-conductor and a three-conductor non-invasive TDR probe. The WRCs measured by the new cell were verified with the results of pressure plate measurements. The WRCs measured by the two-conductor and the three-conductor non-invasive TDR probes were compared and the effects of sampling volume of TDR on the measured WRCs were analysed.

2. Description of the non-invasive TDR-tensiometer cell

Fig. 1 shows the schematic diagram of the non-invasive TDR-tensiometer cell together with a photograph of the experimental setup. The instrument consists of a non-invasive TDR probe printed on a plastic plate (68 mm in diameter and 8 mm in height), a ceramic cup (6 mm in diameter and 5 mm in height), a plastic tube, a pressure gauge, a sample container (70 mm in diameter and 50 mm in height), and a plastic pedestal. A circular groove is introduced in the plastic pedestal to contain the non-invasive TDR probe. In this study, non-invasive TDR probes with different waveguide layouts (i.e., number of conductors and waveguide length) were fabricated and evaluated. Detailed information about the design of non-invasive TDR probes is given in Section 3.1. The non-invasive TDR probe is connected to TDR 100 (Campbell Scientific Co., Ltd) through a 50 Ω coaxial cable. To measure

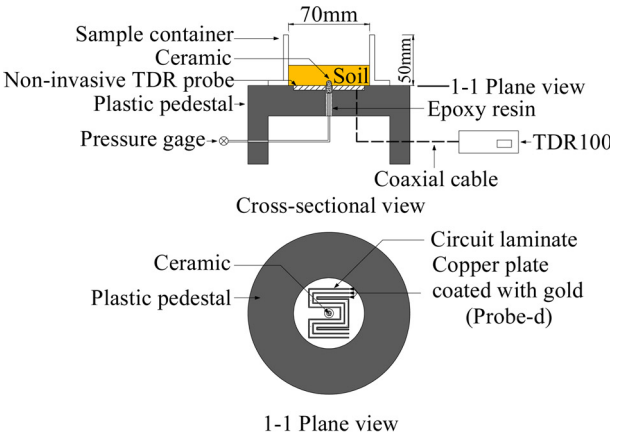

Fig. 1. The new cell equipped with the non-invasive TDR and tensiometer: (a) Schematic diagram; (b) Photograph.

the soil volumetric water content, a pulse generator sends a step pulse along the waveguide to sense the soil medium above the probe. The soil volumetric water content can be calculated through the dielectric permittivity determined from the reflection waveform. More details about the calibration of non-invasive TDR probes are described in Section 4.

On the other hand, the tensiometer consists of a porous ceramic cup, a plastic tube, and a pressure gauge. A hole was drilled in the center of the pedestal where the ceramic cup is inserted. The ceramic cup is fixed in the pedestal using epoxy resin. It should be noted that ceramic cup exposed to the soil is 3 mm high. The ceramic cup is connected to a pressure gauge through a plastic tube. To measure the soil suction, the ceramic cup and plastic tube are first filled in de-aired water and then equilibrium is achieved between the soil and tensiometer. The water in the tensiometer therefore has the same pressure as the pore water in the soil. The pore water pressure of soil is recorded through the pressure gauge. It should be noted that the TDR technique provides measurements of soil water content from completely dry to fully saturated conditions. According to calibration tests, the data of calculated and measured soil water content lie within ± 4 % of the 1:1 line, which indicates the non-invasive TDR probes provide satisfactory accuracy. On the other hand, the tensiometer used in this study measures soil suctions ranging from 0 to 100 kPa, with a resolution of 0.1 kPa.

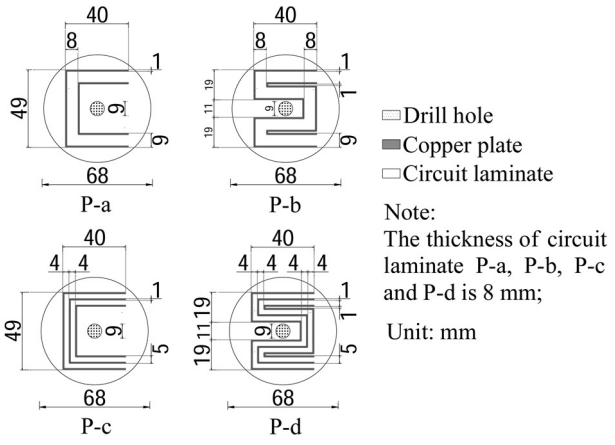

(a)

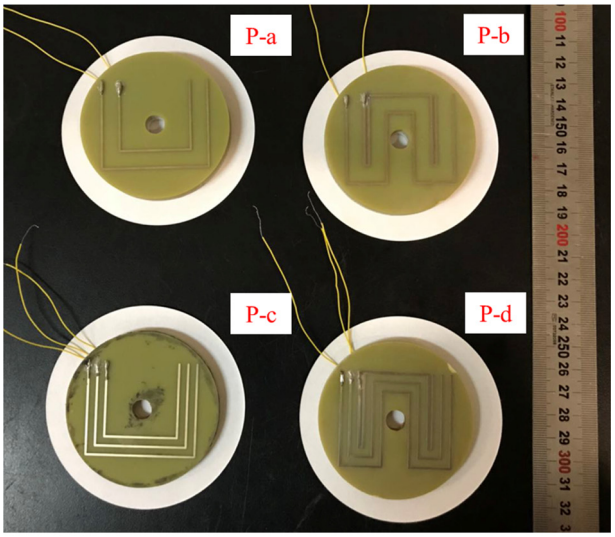

(b)

Fig. 2. Non-invasive TDR probes with different waveguide layouts: (a) Schematic diagram; (b) Photograph.

3. Development of non-invasive TDR probes

3.1. Probe design

Fig. 2 shows the configuration of four trial non-invasive TDR probes together with their photographs. For each of probe, copper waveguides are placed on a non-conductive circuit laminate. The waveguide is configured in a serpentine pattern but with different numbers of copper plates and lengths. To avoid corrosion, a thin layer of gold is coated on the surface of the copper conductors. The two-conductor non-invasive TDR probes (i.e., Probes P-a and P-b) have an average waveguide length of 111 mm and 173 mm, respectively. The thickness and width of the copper conductor of Probes P-a and P-b are 0.02 mm and 1 mm, respectively. The spacing between the two copper plates is 8 mm. The three-conductor non-invasive TDR probes (i.e., Probes P-c and P-d) have an average waveguide length of 111 mm and 173 mm, respectively. The thickness and width of the copper plate of Probes P-c and P-d are identical to P-a and P-b but with a conductor spacing of 4 mm. In addition, the thickness of the circuit laminate for all probes is 8 mm. The production of these probes is similar to the method used in manufacturing printed circuit board (see in Fig. 2b).

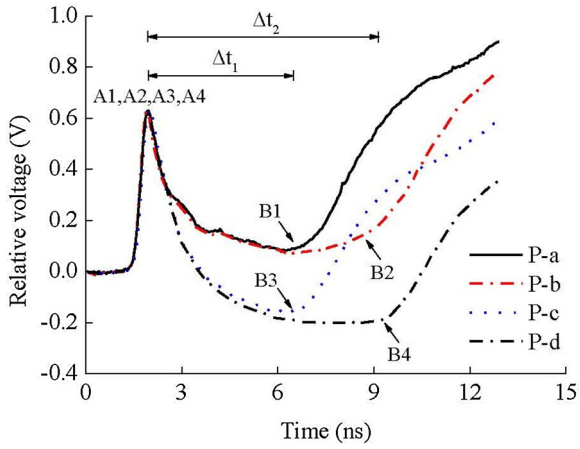

Fig. 3. Waveforms of non-invasive TDR probes with different waveguide layouts.

3.2. Evaluation of the probe performance and characteristics

3.2.1. Reflection waveforms

Fig. 3 shows the reflection waveforms in water for the four trial non-invasive TDR probes. During measurements, a step pulse is sent by the signal generator and propagates along the waveguide. Some of the wave energy is reflected at the beginning of the probe (A1, A2, A3 and A4) due to the impedance mismatch between the coaxial cable and the connector. Following the short positive reflection at the connector is the negative reflection from the interface with the sensing section. The reflection waveforms of Probes P-c and P-d drop down to a lower level than that of Probes P-a and P-b. Compared to the two-conductor probes (i.e., Probes P-a and P-b), the impedances of three-conductor probes (i.e., Probes P-c and P-d) are smaller and hence larger negative reflections are exhibited. The reflection points (B1, B2, B3 and B4) from the end of the probes can also be clearly identified from the reflection waveforms. The round-trip travel time (Δt) of the step pulse in the sensing section can be determined from the reflection points A and B. As expected, the signal travel times of Probes P-a and P-c (Δt_1) or Probes P-b and P-d (Δt_2) are similar because of the same waveguide length. In addition, the Δt_2 is larger than Δt_1 as the waveguides of Probes P-b and P-d are longer than that of Probes P-a and P-c.

The reflection waveforms shown in Fig. 3 suggest that any of the four trial waveguide layouts can be adopted for water content measurements in the aspect of identifying reflection points. However, as the waveguide length increases, the travel time is more sensitive to variation of dielectric permittivity of the surrounding material (Lin et al., 2006). Therefore, Probes P-b and P-d were adopted in the following study.

3.2.2. Measurement sensitivity

The dielectric permittivity measured by a non-invasive TDR probe is a weighted average dielectric permittivity of the target material and the circuit laminate. Placing serpentine conductors on the surface of circuit laminate allows the waveguide to non-invasively sense the soil above it, but decreases the sensitivity of dielectric permittivity measurements. The optimal design of non-invasive TDR probe would minimize the contribution from the circuit laminate to the measured dielectric permittivity, thereby maximizing the measurement sensitivity to the target material. The measurement sensitivity of Probes P-b and P-d can be evaluated through the mixing model proposed by Birchak et al. (1974):

$$(\varepsilon_{a,eff})^n = w(\varepsilon_{a,tm})^n + (1-w)(\varepsilon_{a,cl})^n \quad (1)$$

where $\varepsilon_{a,eff}$ is the dielectric permittivity measured by the non-invasive TDR probe; $\varepsilon_{a,tm}$ and $\varepsilon_{a,cl}$ are the dielectric permittivity of target material and circuit laminate, respectively; the exponent n is a shape factor

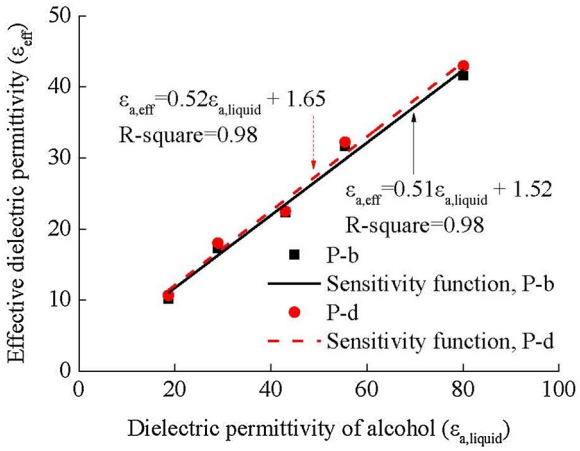

Fig. 4. Measurement sensitivity of Probes P-b and P-d.

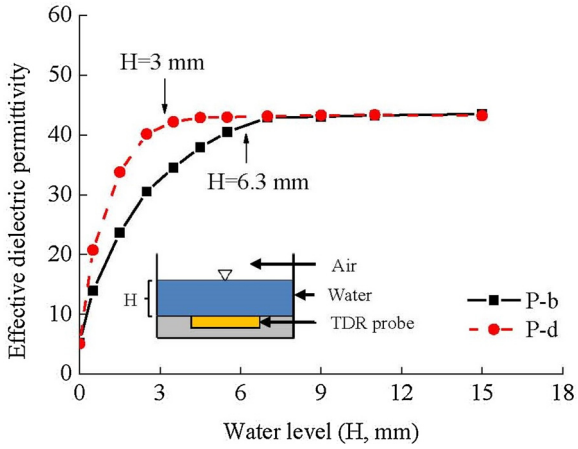

Fig. 5. Vertical sampling range of dielectric permittivity measurements for Probes P-b and P-d.

ranging from −1 to 1, where $n = 1$ if the medium is a parallel combination of capacitors and $n = -1$ for a series connection of capacitors (Lin et al., 2006); w is the weighting factor representing the percentage contribution of the target material to the measured dielectric permittivity. According to Ferre et al. (1998), the distribution of medium could be considered as capacitors in parallel if the dielectric permittivity is a function of the distribution of electrostatic potential only. The design of the parallel connection of capacitors for a TDR probe could be achieved by placing the material (e.g., circuit laminate) in parallel with the target material (e.g., soil) with respect to the metal rod of the waveguide (Lin et al., 2006). In this study, since the target material and circuit laminate are placed in parallel to surround the copper waveguide, the value of parameter n is theoretically equal to 1.

To experimentally calibrate the probe parameters in Eq. (1), some target materials were prepared by mixing the ethanol with deionized water to different volume fractions ($V_{ethanol}/V_{water} = 0 \sim 1$). After each of the mixture was prepared, the $\varepsilon_{a,tm}$ and $\varepsilon_{a,eff}$ were measured through a conventional three-rod TDR probe and the non-invasive TDR probe, respectively. The measured $\varepsilon_{a,tm}$ and $\varepsilon_{a,eff}$ were fit to the mixing model to determine the weighting factor (w) of Probes P-b and P-d. Fig. 4 shows the relationship between $\varepsilon_{a,eff}$ and $\varepsilon_{a,tm}$ for Probes P-b and P-d. The results indicate a good relationship between $\varepsilon_{a,eff}$ and $\varepsilon_{a,tm}$ with high values of R^2 (0.98). The weighting factors of Probes P-b and P-d are 0.51 and 0.52, respectively. It shows that the weighting factor of the non-invasive TDR probe is independent of the number of copper conductors. It is therefore that Probes P-b and P-d show similar measurement sensitivity, in which the target material contributes around 50% to the effective (measured) dielectric permittivity. In the aspect of measurement sensitivity, the performances of the two probes are comparable. The measurement sensitivity of 50% is attributed to the design of the non-invasive TDR probe, in which the waveguide is sandwiched between the circuit laminate and the target material. Therefore, half of the space around the probe is in contact with the measured zone.

3.2.3. Vertical sampling range of dielectric permittivity

Soil particles and water within a soil sample may be heterogenous. It is therefore that the sampling volume of a TDR probe should be large enough to ensure that the measured soil water content is representative to that of the whole sample. The sampling volume of a TDR probe can be calculated through the weighting function concept proposed by Knight (1992) and the numerical approach of Knight et al. (1997). Since the calculation of the sampling volume of a 3D non-invasive TDR probe is rather complicated and also needs to be verified experimentally. An experimental approach, similar to that proposed by Lin et al. (2006), was adopted to determine the vertical sampling range of Probes P-b and P-d for the dielectric permittivity measurement.

The schematic diagram of the experimental setup is illustrated in Fig. 5. The sample container was filled with water at different water levels. Within the sensing range is a composite medium composed of air and water, whose dielectric permittivity are the two opposite extremes (i.e., $\varepsilon_{a,air} = 1$ and $\varepsilon_{a,water} = 80$). The water level ($H = 15$ mm) was initially high enough to ensure that the dielectric permittivity measured by the non-invasive TDR probes is an averaged value of the circuit laminate and the water. The water level was then drawn down in steps. The decrease of water level results in a replacement of water with air within the vertical sampling range of the non-invasive probes. The vertical sampling range of Probes P-b and P-d can be determined as the height of water where the measured dielectric permittivity exhibits a sharp decrease.

Fig. 5 also includes the relationship between the water level and the measured dielectric permittivity from Probes P-b and P-d. For Probe P-b, the measured dielectric permittivity approaches to a constant value when water level is greater than 3 mm. This implies that the target material located at the height greater than 3 mm has minuscule effect on the effective dielectric permittivity measured by Probe P-b. As the water level drops from 3 mm to zero, the measured dielectric permittivity decreases significantly. The above experimental results indicate that the majority of the response of Probe P-b occurs within the first 3 mm above the sensing waveguide. For Probe P-d, the variation of dielectric permittivity with water level shows a similar pattern to that of Probe P-b. A sharp decrease of the measured dielectric permittivity occurs when the water level drops to 6.3 mm. In comparison, Probe P-b has a sampling range two times greater than Probe P-d. This result is consistent with previous numerical studies (Ferre et al., 1998), showing that three-conductor TDR probe has a smaller sampling volume than that of two-conductor TDR probe. It should be noted that the sampling height was independent of tested material because the design of the non-invasive TDR probe falls into the category of parallel connection of capacitors (Ferre et al., 1998; Lin et al., 2006).

4. Calibration for water content measurement

Remolded loess samples with different water contents were used to calibrate the relationship between the measured soil volumetric water content and dielectric permittivity for Probes P-b and P-d. The preparation of remolded soils is introduced in detail in Section 5.2. The prepared soil sample was placed on the newly developed cell to measure the dielectric permittivity. After measuring the soil dielectric permittivity ($\varepsilon_{a,soil}$), the water content of the remolded loess was measured by oven-dry method following the ASTM D2216 (2005) procedure. The presence of the porous ceramic cup (and water contained inside) would influence the water content measurements by the non-

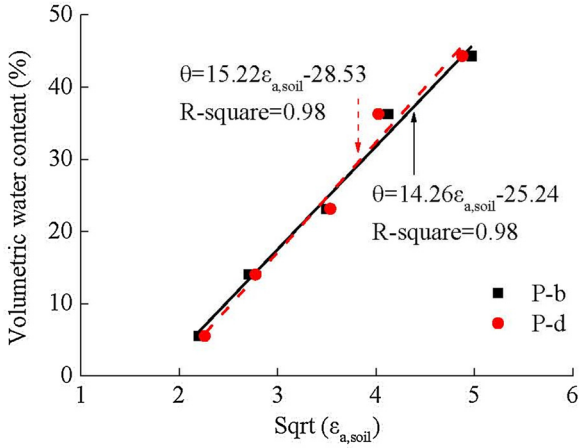

Fig. 6. Calibrated relationships between $\sqrt{\varepsilon}_{a,soil}$ and volumetric water content for Probes P-b and P-d.

invasive TDR probe. It should be noted that the calibration of the non-invasive TDR probe was performed with the porous ceramic cup to be under the same condition as in subsequent measurements.

Fig. 6 shows the calibrated relationships between soil volumetric water content and $\sqrt{\varepsilon}_{a,soil}$ for Probes P-b and P-d. $\varepsilon_{a,soil}$ is calculated through the equations shown in Fig. 4 from the effective dielectric permittivity ($\varepsilon_{a,eff}$) measured by Probes P-b and P-d. For both Probes P-b and P-d, the measured soil dielectric permittivity decreases with decreasing soil volumetric water content. Furthermore, good linear relationships between soil volumetric water content and $\sqrt{\varepsilon}_{a,soil}$ are obtained with high values of R^2 (0.98). The linear relationship between $\sqrt{\varepsilon}_{a,soil}$ and θ was also used by previous studies for calibrating the TDR measurements (Yu and Drnevich, 2004; Lin et al., 2006). The calibrated parameters (i.e., slope and intercept) in this work are slightly different from previous studies because of different soil types tested.

5. WRC of loess by transient evaporation method

5.1. Tested material

In this study, the WRCs of undisturbed and remolded loess were measured with Probes P-b and P-d by the transient evaporation method and the pressure plate test. Cubic loess blocks 0.2 m × 0.2 m × 0.2 m in dimension were collected from an excavated pit in Xi'an, China. The particle size distribution of the test loess is shown in Fig. 7. It consists of 75.8% silt (0.002-0.063 mm) and 24.2% clay (< 0.002 mm). On the other hand, the measured liquid limit and plastic limit of the test loess

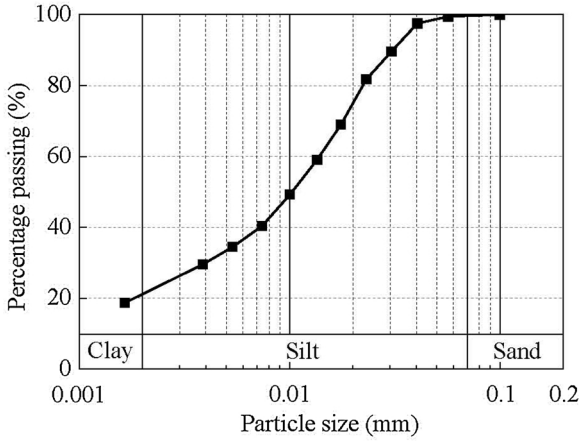

Fig. 7. Particle size distribution of the tested loess.

Table 1
Soil properties of the tested loess.

Parameter	Value
Specific gravity	2.69
Dry density (kg/m^3)	1523
Gravimetric water content (%)	16.6
Liquid limit (%)	35.7
Plastic limit (%)	16.2
Particle size distribution (%)	–
Sand content (0.075–2 mm)	0
Silt content (0.002–0.075 mm)	78.8
Clay content (≤0.002 mm)	21.2
Unified soil classification (ASTM D2487)	CL

are 35.7% and 16.2%, respectively. According to the ASTM D2487 (2011), the tested loess is classified as clay with low plasticity (CL). More detailed physical properties of the tested loess are summarized in Table 1.

5.2. Sample preparation method

Both undisturbed and remolded loess soils were tested in this study. To prepare undisturbed loess specimens, an oedometer ring (70 mm in diameter and 19 mm in height) was pushed into the loess block. The top and bottom of the specimen were trimmed with a wire saw. According to previous studies (Atkinson et al., 1992; Ng et al., 2016), sample disturbance is minimised when this method of sample preparation is used. The dry density and water content of the undisturbed sample were measured to be 1523 kg/m^3 and 16.6%, respectively. For the remolded sample, the loess soils were firstly oven-dried and then passed through a 2 mm British Standard (BS) sieve. The prepared soils were evenly spread on a plastic plate and de-aired water was sprayed on the soils to slightly increase the water content. The mixture was mixed thoroughly with a blender until it reached the gravimetric water content of 16.6% same as the undisturbed loess specimen. The loess grains were compacted into an oedometer ring by the static compaction method to reach a dry density of 1523 kg/m^3 same as the undisturbed loess specimen.

5.3. Experimental procedure

The undisturbed and remolded loess samples were first saturated in a vacuum chamber following the procedure similar to the ASTM D6836. A small circular hole (3 mm in height and 6 mm in diameter) was drilled in the centre of the specimen where the ceramic cup was inserted. The soil specimen was carefully moved into the measurement cell to ensure a good contact between the soil and the measurement instruments (i.e., the non-invasive TDR probe and the tensiometer). The soil specimen was dried by exposing its top surface to the atmosphere. The readings of the pressure gauge and non-invasive TDR probes were recorded in a series of steps to measure the WRC along the drying path. Fig. 8 shows the changes in water mass and suction during the transient evaporation. The average evaporation rate adopted in this study is 0.34 g/h, which is slightly smaller than the transient evaporation tests carried out by Lourenco et al. (2011) (i.e., 0.39 g/h) and Chen et al. (2015) (i.e., 0.37 g/h). This is probably because that the specimen tested in this study is 1.2 times denser than that of their specimens and hence exhibits a smaller permeability. On the other hand, the measured soil suction increases nonlinearly from zero to 95 kPa during evaporation. It should be noted that the suction variation curve exhibits a plateau at the end of the evaporation. Previous studies also showed that the measurements of tensiometer are not reliable at high suctions (e.g., > 80 kPa) because of cavitation (Fredlund and Rahardjo, 1993; Cui et al., 2007). The tests in the following study were stopped when the reading of tensiometer reached 80 kPa, which approaches to the air

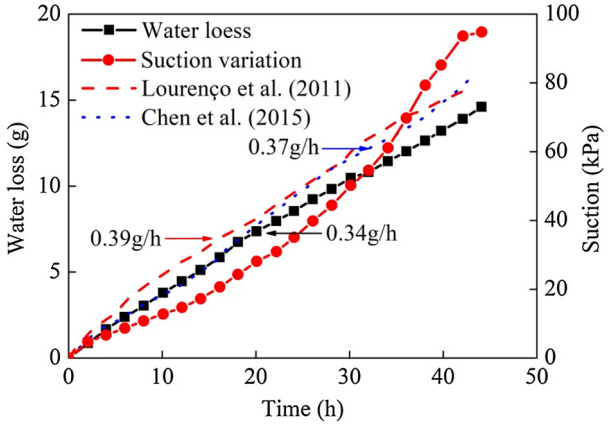

Fig. 8. Changes in the water mass and suction during evaporation.

entry value (AEV) of ceramic cup (i.e., 100 kPa).

In addition, the WRCs of undisturbed and remolded loess samples were also measured through the conventional pressure plate tests. The soil samples were placed on the ceramic disk of a pressure plate chamber. The air pressure inside the chamber was increased in a series of steps. It should be noted that 5–10 days were required to achieve equilibrium between the soil specimen and the pressure plate at a given pressure. After suction equalization, the soil sample was removed from the pressure chamber to measure the volumetric water content with an electronic balance. The soil height and diameter was also measured with a vernier caliper during pressure plate measurements. It was found that the volume changes of tested specimens were almost negligible at the suction range considered in this study (i.e., 0–100 kPa). Therefore, the soil volumetric water contents were determined with an assumption of constant soil volume.

5.4. Analyses of results

Fig. 9a shows the WRCs of undisturbed loess measured by the pressure plate and the transient evaporation method with Probes P-b and P-d. The result from the pressure plate measurement provides a benchmark to verify the performance of the non-invasive TDR probes. According to the results, the three measured WRCs share a similarly nonlinear pattern. The soil volumetric water content remains constant at low suction and then decreases dramatically when the suction is beyond the AEV. The AEV of each soil specimen was estimated by extending a line from the constant slope portion of the water retention curve to intersect the suction axis at the saturated condition (Vanapalli et al., 1996). Furthermore, WRCs measured by the pressure plate test and the transient evaporation method with Probe P-d are in fairly good agreement. Compared to the WRC measured by the pressure plate, the WRC measured by Probe P-b underestimates the soil volumetric water content when the suction is beyond the AEV (i.e., 3.5 kPa). This is probably due to the fact that a water content gradient is induced across the sample height when the transient evaporation acts from the soil top surface (Fredlund and Rahardjo, 1993). The water content at the top is expected to be lower than that at the bottom. The vertical sampling range of water content measurement using Probe P-d is similar to that of the suction measurement using the tensiometer (i.e., 3 mm). However, the vertical sampling range of Probe P-b (i.e., 6.3 mm) is two times larger than that of the tensiometer (i.e., 3 mm). At a given transient state, the measured average volumetric water content within the sampling volume of Probe P-b is smaller than that of Probe P-d.

Fig. 9b shows the WRCs of remolded loess measured by the pressure plate and the transient evaporation method with Probes P-b and P-d. Similar to the undisturbed loess, the soil volumetric water content also decreases nonlinearly with increasing suction for each WRC. The WRC of remolded loess measured by the Probe P-d is also in good agreement

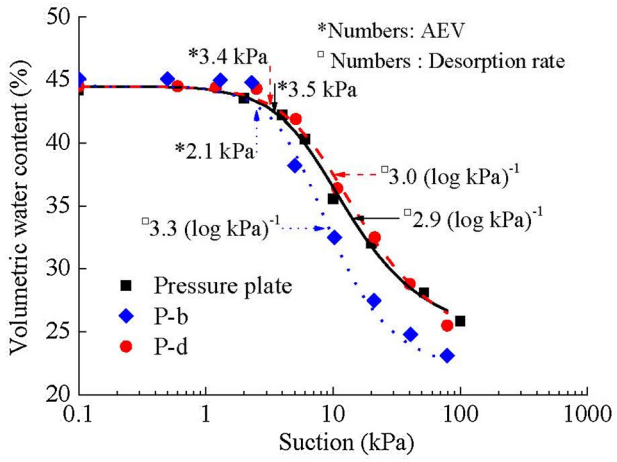

(a)

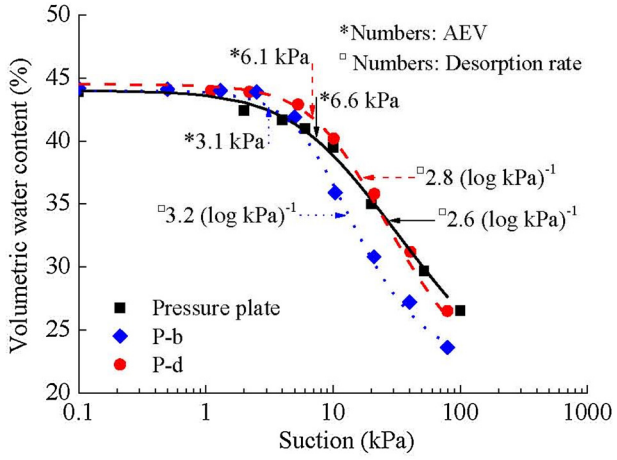

(b)

Fig. 9. Comparisons of WRCs measured by the pressure plate and transient evaporation method with Probes P-b and P-d: (a) undisturbed loess specimen; (b) remolded loess specimen.

with the result of pressure plate measurement, while the result of Probe P-b underestimates the water content at a given suction. As explained above, the different performance between Probes P-b and P-d for measuring the WRC of remolded loess can be attributed to their different sampling volumes.

To further analyse the WRC quantitatively, the model proposed by Van Genuchten (1980) is adopted to fit the measured WRCs.

$$\theta = \theta_r + \frac{\theta_s - \theta_r}{[1 + (\alpha s)^n]^m} \quad (2)$$

where θ is the volumetric water content; s is the suction; θ_r and θ_s represent the residual volumetric water content and the saturated volumetric water content, respectively; a, n and m are the soil parameters. According to previous studies (Van Genuchten, 1980; Mu et al., 2018), a relationship between n and m can be established as: $n = 1\text{-}1/m$.

For both the undisturbed and remolded loess samples, the least-square curve-fitting technique was adopted to obtain the parameters θ_r, a, n and m. The parameters derived from the curve fitting are summarized in Table 2. The van-Genuchten model works well in fitting the WRCs measured by the pressure plate and the transient evaporation method, as indicated by the high values of R^2 (0.99). The differences in

Table 2
Summary of the parameters derived from the curve fitting.

Soil specimen	WRC measured by the pressure plate					WRC measured by Probe P-d					WRC measured by Probe P-b				
	θ_r	a	n	m	R^2	θ_r	a	n	m	R^2	θ_r	a	n	m	R^2
Undisturbed	24.5	0.14	1.92	0.48	0.99	21.8	0.16	2.25	0.56	0.99	23.3	0.12	1.84	0.46	0.99
Remolded	15.0	0.10	1.40	0.29	0.99	21.4	0.12	2.01	0.50	0.99	17.7	0.08	1.67	0.40	0.99

the AEV and desorption rate between the WRC determined by Probe P-d and that by the pressure plate measurement are less than 10% for both undisturbed and remolded loess samples. On the other hand, the AEV of the undisturbed and remolded loess specimens determined by Probe P-b is 66.7% and 112.9% smaller than that of the result determined by pressure plate, respectively. It is noteworthy that the AEV of remolded loess (6.6 kPa) is about twice larger than that of undisturbed loess (3.5 kPa). Extra-large pores (e.g., about 0.5 mm in diameter) were observed in the undisturbed loess by naked eye. The extra-large pores in undisturbed loess may arise in the initial deposition or subsequent biological actions (e.g., plant root and worm) (Wang et al., 2018). For the remolded sample, extra-large pores were eliminated because of the uniform compaction during specimen preparation process. According to a previous study (Ng et al., 2016), the specimen with extra-large pores may require a smaller air pressure to allow air to break into soil pores.

6. Discussions

Transient evaporation method is promising for rapid determination of soil WRC through simultaneously measuring soil volumetric water content and suction. In this study, a new cell consisting of a non-invasive TDR probe and a tensiometer was developed to measure the WRC of both structured and remolded soil during transient evaporation. The newly developed cell was especially applicable to measure the WRC of structured soils because of no sample disturbance induced by the penetration of moisture probe. According to the experimental results of this study, the sampling volume of the moisture probe should be compliant with that of the tensiometer to ensure an accurate measurement of soil WRC using the transient evaporation method. Although the pattern of soil WRC can be captured through a moisture probe and a tensiometer with different sampling volumes, the measured soil WRC deviates from the result of pressure plate measrement significantly (see in Fig. 9). On the contrary, the soil WRC obtained from a moisture probe and a tensiometer with compliant sampling volumes is similar to that of the results of pressure plate measurements (see in Fig. 9). On the other hand, the evaporation rate of soil specimen may be another key factor influencing the measurement accuracy of soil WRC using the transient evaporation method. This is mainly because of the different response times between the moisture probe and the tensiometer. The measurement of soil suction through a tensiometer has a slower response than the water content measurements through a moisture probe. To measure the soil suction, it takes a few seconds for the equalization between the soil and the saturated porous ceramic cup (AEV: 1 bar). Therefore, the evaporation rate should be slow enough to ensure that the measurements of water content keep pace with that of soil suction. In this study, an evaporation rate of 0.34 g/h was found to be appropriate to measure the WRCs of undisturbed and remolded loess using the transient method.

7. Conclusions

In an effort to improve the efficiency of WRC measurements for structured soils, non-invasive TDR probes were developed to construct a new measurement cell together with a tensiometer for transient evaporation method. The following conclusions may be drawn from the experimental results:

(i) The non-invasive TDR probe developed by placing serpentine waveguide on the circuit laminate is effective in measuring the volumetric water content of structured loess without sample disturbance. The TDR reflection points can be clearly identified for all waveguide layouts tested (i.e., number of conductors and conductor length). Furthermore, the target material placed on the above of the non-invasive TDR probe contributes approximately 50% to the measured dielectric permittivity.
(ii) The WRCs of undisturbed and remolded loess measured with Probe P-d (three-conductor waveguide) are in good agreement with the results measured by the pressure plate tests, while the results of Probe P-b (two-conductor waveguide) underestimate the soil water content for a given suction. This is because Probe P-d and the tensiometer share a similar vertical sampling range for both soil volumetric water content and suction measurements. On the other hand, the vertical sampling range of Probe P-b is about two times larger than that of the tensiometer. At a given soil suction, a smaller average soil volumetric water content is measured by Probe P-b because of the water content gradient induced by transient evaporation.

Declaration of Competing Interest

We declare that we do not have any commercial or associative interest that represents a conflict of interest in connection with the work submitted.

Acknowledgement

This work was supported by the opening fund of MOE Key laboratory of Soft Soils and Geoenvironmental Engineering (2018P04); The National Science Fund for Distinguished Young Scholars (51625805); the National Science Foundation of China (51909205); the China Postdoctoral Science Foundation (2018M631166; 2019T120914); the Fundamental Research Fund for the Central Universities of China (xjj2018250) and the innovative talents promotion plan in Shaanxi Province (2018KJXX-033).

References

ASTM D2487, 2011. Standard practice for classification of soils for engineering purposes (unified soil classification system). Annnual Book of ASTM Standards. ASTM International, West Conshohocken, PA.
ASTM D2216, 2005. Standard test methods for laboratory determination of Water (moisture) content of soil and Rock by mass. Annnual Book of ASTM Standards. ASTM International, West Conshohocken, PA.
Atkinson, J.H., Allman, M.A., Böese, R.J., 1992. Influence of laboratory sample preparation procedures on the strength and stiffness of intact Bothkennar soil recovered using the Laval sampler. Gotechnique 42 (2), 349–354.
Birchak, J.R., Gardner, C.G., Hipp, J.E., Victor, J.M., 1974. High dielectric constant microwave probes for sensing soil moisture. Proc. Ieee 62, 93–98.
Cui, Y., Jiang, Y., Guo, C., 2019. Investigation of the initiation of shallow failure in widely graded loose soil slopes considering interstitial flow and surface runoff. Landslides 16 (4), 815–828.
Cui, Y.J., Tang, A.M., Mantho, A.T., De Laure, E., 2007. Monitoring field soil suction using a miniature tensiometer. Geotech. Test. J. 31 (1), 95–100.
Ferre, P.A., Knight, J.H., Rudolph, D.L., Kachanoski, R.G., 1998. The sample areas of conventional and alternative time domain reflectometry probes. Water Resour. Res. 34 (11), 2971–2979.
Fredlund, D.G., Rahardjo, H., 1993. Soil Mechanics for Unsaturated Soils. John Wiley & Sons, Inc., New York, N. Y.

Han, Z., Vanapalli, S.K., 2016. Stiffness and shear strength of unsaturated soils in relation to soil-water characteristic curve. Géotechnique 66 (8), 627–647.
Haeri, S.M., Khosravi, A., Garakani, A.A., Ghazizadeh, S., 2016. Effect of soil structure and disturbance on hydromechanical behavior of collapsible loessial soils. Int. J. Geomech. 17 (1), 04016021.
Hou, X., Vanapalli, S.K., Li, T., 2018. Water infiltration characteristics in loess associated with irrigation activities and its influence on the slope stability in Heifangtai loess highland, China. Eng. Geol. 234, 27–37.
Knight, J.H., 1992. Sensitivity of time domain reflectometry measurements to lateral variations in soil water content. Water Resour. Res. 28 (9), 2345–2352.
Knight, J.H., Ferré, P.A., Rudolph, D.L., Kachanoski, R.G., 1997. A numerical analysis of the effects of coatings and gaps upon relative dielectric permittivity measurement with time domain reflectometry. Water Resour. Res. 33 (6), 1455–1460.
Krisdani, H., Rahardjo, H., Leong, E.C., 2009. Use of instantaneous profile and statistical methods to determine permeability functions of unsaturated soils. Can. Geotech. J. 46 (7), 869–874.
Lin, C.P., Tang, S.H., Chung, C.C., 2006. Development of TDR penetrometer through theoretical and laboratory investigations: 1. Measurement of soil dielectric permittivity. Geotech. Test. J. 29 (4), 306–313.
Lourenco, S.D.N., Gallipoli, D., Toll, D.G., Augarde, C.E., Evans, F.D., 2011. A new procedure for the determination of soil-water retention curves by continuous drying using high-suction tensiometers. Can. Geotech. J. 48 (2), 327–335.
Mitchell, J.K., Soga, K., 2005. Fundamentals of Soil Behavior, 3rd ed. John Wiley & Sons, New York, NY, USA.
Mu, Q.Y., Zhou, C., Ng, C.W.W., Zhou, G.G.D., 2019. Stress effects on soil freezing characteristic curve: equipment development and experimental results. Vadose Zone J. 18, 180199.
Mu, Q.Y., Ng, C.W.W., Zhou, C., Zhou, G.G.D., Liao, H.J., 2018. A new model for capturing void ratio-dependent unfrozen water characteristics curves. Comput. Geotech. 101, 95–99.
Ng, C.W.W., Mu, Q.Y., Zhou, C., 2016. Effects of soil structure on the shear behaviour of an unsaturated loess at different suctions and temperatures. Can. Geotech. J. 54 (2), 270–279.
Ng, C.W.W., Leung, A.K., 2011. Measurements of drying and wetting permeability functions using a new stress-controllable soil column. J. Geotech. Geoenviron. Eng. 138 (1), 58–68.
Nissen, H.H., Ferré, P.A., Moldrup, P., 2003. Metal-coated printed circuit board time domain reflectometry probes for measuring water and solute transport in soil. Water Resour. Res. 39 (7), 1184.
Rassam, D.W., Williams, D.J., 2000. A dynamic method for determining the soil water characteristic curve for coarse-grained soils. Geotech. Test. J. 23 (1), 67–71.
Selker, J.S., Graff, L., Steenhuis, T., 1993. Noninvasive time domain reflectometry moisture measurement probe. Soil Sci. Soc. Am. J. 57 (4), 934–936.
Singh, D.N., Kuriyan, S.J., 2003. Estimation of unsaturated hydraulic conductivity using soil suction measurements obtained by an insertion tensiometer. Can. Geotech. J. 40 (2), 476–483.
Su, W., Cui, Y.J., Qin, P.J., Zhang, F., Ye, W.M., Conil, N., 2018. Application of instantaneous profile method to determine the hydraulic conductivity of unsaturated natural stiff clay. Eng. Geol. 243 (4), 111–117.
Subedi, S., Kawamoto, K., Karunarathna, A.K., Moldrup, P., Wollesen de Jonge, L., Komatsu, T., 2013. Mini tensiometer-time domain reflectometry coil probe for measuring soil water retention properties. Soil Sci. Soc. Am. J. 77 (5), 1517–1528.
Vanapalli, S.K., Fredlund, D.G., Pufahl, D.E., Clifton, A.W., 1996. Model for the prediction of shear strength with respect to soil suction. Can. Geotech. J. 33 (3), 379–392.
Van Genuchten, M.T., 1980. A closed-form equation for predicting the hydraulic conductivity of unsaturated soils. Soil Sci. Soc. Am. J. 44 (5), 892–898.
Vaz, C.M., Hopmans, J.W., Macedo, A., Bassoi, L.H., Wildenschild, D., 2002. Soil water retention measurements using a combined tensiometer-coiled time domain reflectometry probe. Soil Sci. Soc. Am. J. 66 (6), 1752–1759.
Wang, W., Wang, Y., Sun, Q., Zhang, M., Qiang, Y., Liu, M., 2018. Spatial variation of saturated hydraulic conductivity of a loess slope in the South Jingyang Plateau China. Eng. Geol. 236, 70–78.
Xu, L., Dai, F.C., Tham, L.G., Tu, X.B., Min, H., Zhou, Y.F., Wu, C.X., Xu, K., 2011. Field testing of irrigation effects on the stability of a cliff edge in loess, North-west China. Eng. Geol. 120 (1–4), 10–17.
Yu, X., Drnevich, V.P., 2004. Soil water content and dry density by time domain reflectometry. J. Geotech. Geoenviron. Eng. 130 (9), 922–934.
Zhan, T.L.T., Mu, Q.Y., Chen, Y.M., Ke, H., 2015. Evaluation of measurement sensitivity and design improvement for time domain reflectometry penetrometers. Water. Resour. Res. 51 (4), 2994–3006.
Zhai, Q., Rahardjo, H., 2015. Estimation of permeability function from the soil–water characteristic curve. Eng. Geol. 199, 148–156.
Zhang, N., Yu, X., Pradhan, A., 2017. Application of a thermo-time domain reflectometry probe in sand-kaolin clay mixtures. Eng. Geol. 216, 98–107.